Development 140, 1055-1066 (2013) doi:10.1242/dev.090860

The transcription factor Otx2 regulates choroid plexus development and function

Pia A. Johansson[1], Martin Irmler[2], Dario Acampora[3,4], Johannes Beckers[2,5], Antonio Simeone[3,4] and Magdalena Götz[1,6,*]

SUMMARY

The choroid plexuses (ChPs) are the main regulators of cerebrospinal fluid (CSF) composition and thereby also control the composition of a principal source of signaling molecules that is in direct contact with neural stem cells in the developing brain. The regulators of ChP development mediating the acquisition of a fate that differs from the neighboring neuroepithelial cells are poorly understood. Here, we demonstrate in mice a crucial role for the transcription factor Otx2 in the development and maintenance of ChP cells. Deletion of *Otx2* by the Otx2-CreERT2 driver line at E9 resulted in a lack of all ChPs, whereas deletion by the Gdf7-Cre driver line affected predominately the hindbrain ChP, which was reduced in size, primarily owing to an increase in apoptosis upon *Otx2* deletion. Strikingly, Otx2 was still required for the maintenance of hindbrain ChP cells at later stages when *Otx2* deletion was induced at E15, demonstrating a central role of Otx2 in ChP development and maintenance. Moreover, the predominant defects in the hindbrain ChP mediated by Gdf7-Cre deletion of *Otx2* revealed its key role in regulating early CSF composition, which was altered in protein content, including the levels of Wnt4 and the Wnt modulator Tgm2. Accordingly, proliferation and Wnt signaling levels were increased in the distant cerebral cortex, suggesting a role of the hindbrain ChP in regulating CSF composition, including key signaling molecules. Thus, Otx2 acts as a master regulator of ChP development, thereby influencing one of the principal sources of signaling in the developing brain, the CSF.

KEY WORDS: Cerebral cortex development, Cerebrospinal fluid, Wnt, Mouse

INTRODUCTION

The local environment, the niche, plays a key role in regulating neural stem and progenitor behavior and identity during development (Johansson et al., 2010). As cerebrospinal fluid (CSF) contains a variety of signaling factors (Parada et al., 2008, Gato and Desmond, 2009; Huang et al., 2010; Johansson et al., 2010; Lehtinen et al., 2011) its composition might contribute to the unique niche environment of the neural stem cells lining the ventricle (Johansson et al., 2010).

In the adult and during development the composition of CSF is predominantly determined by the activities of the four choroid plexuses (ChPs) suspended in the cerebral ventricles (Fig. 1A). The ChPs are formed between embryonic day (E) 11 and 14 in the mouse, with the fourth ventricular (hindbrain) ChP differentiating first followed by the two lateral ventricular and later the third ventricular ChP (Dziegielewska et al., 2001). The ChPs acquire barrier, secretory and transport capacities shortly after formation (Møllgård et al., 1976; Ek et al., 2003; Johansson et al., 2005; Johansson et al., 2006; Liddelow et al., 2009; Ek et al., 2010). This early functionality and their localization inside the cerebral ventricles, together with their appearance during the period of neurogenesis, make them uniquely suited for influencing CSF composition and thereby regulating development of the neural stem cells that are in contact with the ventricle along the entire neuraxis (e.g. Götz and Huttner, 2005). In particular, the fourth ventricular ChP, being the first to appear, might initially regulate the composition of the entire CSF, prior to the appearance of the other ChPs and the start of directed CSF bulk flow and reabsorption.

The role of the ChPs in brain development is still largely unknown, as are the factors that regulate ChP development, although it has been shown that BMP and Notch signaling pathways are initially involved in their development (Hébert et al., 2002; Hunter and Dymecki, 2007; Imayoshi et al., 2008). In the early developing chick embryo, reciprocal inhibition between the neuroepithelial transcription factor Emx2 and Otx2 expressed in the dorsal roof plate plays a role in specifying neuroepithelial versus ChP territories (von Frowein et al., 2006). As Otx2 also acts as a potent fate determinant in other parts of the developing mouse brain (Acampora et al., 1995; Puelles et al., 2004) we set out to elucidate its role in ChP specification and development by genetic deletion of *Otx2* in the mouse brain using the novel Otx2-CreERT2 and the Gdf7-Cre mouse lines. These experiments revealed an absolute requirement of Otx2 in ChP development and a novel role of the ChP as a modulator of Wnt signaling mediated via the CSF.

MATERIALS AND METHODS

Animals

All animals were kept in the animal facility of the Helmholtz Center Munich. The day of the vaginal plug was counted as E0. The developmental age was confirmed by measurements of crown-rump length. All experimental procedures were performed in accordance with German and European Union guidelines. The following mouse lines were used: *Otx2* floxed (Puelles et al., 2003), Gdf7-Cre (Lee et al., 2000), TG(Fos-lacZ)34Efu/J Wnt reporter (DasGupta and Fuchs, 1999) and CAG-GFP reporter (Nakamura et al., 2006). We also created a novel mouse line, Otx2-CreERT2 (supplementary material Fig. S1), by replacing the genomic

[1]Helmholtz Center Munich, German Research Center for Environmental Health, Institute for Stem Cell Research, Neuherberg, 85764 Munich, Germany. [2]Helmholtz Center Munich, German Research Center for Environmental Health, Institute for Experimental Genetics, Neuherberg, 85764 Munich, Germany. [3]Institute of Genetics and Biophysics, A. Buzzati-Traverso, CNR Via P. Castellino 111, 80131 Naples, Italy. [4]IRCCS Neuromed, 86077 Pozzilli (IS), Italy. [5]Technical University Munich, Center of Life and Food Sciences Weihenstephan, 85354 Freising, Germany. [6]Physiological Genomics, University of Munich, 80336 Munich, Germany.

*Author for correspondence (magdalena.goetz@helmholtz-muenchen.de)

Accepted 19 December 2012

region spanning the entire *Otx2* coding sequence with the tamoxifen-inducible CreERT2 recombinase followed by the *Otx2* 3′UTR and polyadenylation signal (Feil et al., 1997). The Otx2-CreERT2 mice were treated with 0.1 mg/g body weight tamoxifen (Sigma) in order to induce recombination. Tamoxifen was dissolved in corn oil and administered once to the pregnant mother via oral gavage.

Tissue processing

Whole heads and bodies (E11-13) and brains [E14, E20 and postnatal day (P) 2] were fixed by immersion in 4% (w/v) paraformaldehyde in phosphate-buffered saline (PBS). P7 brains were first perfused with the same fixative followed by immersion. The heads and brains were washed in PBS and immersed in 30% sucrose (w/v in PBS). The tissue was then embedded in Tissue-Tek OCT Compound and frozen on dry ice and cut (cryostat, 12-20 μm) and stored at −20°C.

Immunohistochemistry

Frozen sections were thawed and washed in PBS followed by blocking solution (0.5% Triton X-100, 10% normal goat serum in PBS). The sections were incubated in primary antibodies: rabbit anti-Otx2 (1:200, Chemicon), goat anti-Otx2 (1:600, R&D Systems), chick anti-GFP (1:1000, Aves), rabbit anti-phospho-histone H3 (PH3, 1:400, Millipore), rabbit anti-Pax6 (1:500, Chemicon), rat anti-Pecam/CD31 (Pecam1 – Mouse Genome Informatics) (1:30, BD Pharmingen), rat anti-prominin 1 (1:500, eBiosciences), rabbit anti-cyclin D1 (1:20, Thermoscientific), rabbit anti-β-galactosidase (1:5000, MP Biologicals), rabbit anti-Tbr1 (1:200, Abcam), rat anti-Ctip2 (Bcl11b – Mouse Genome Informatics) (1:200, Abcam) and rabbit anti-Cux1 (1:200, Santa Cruz). The sections were washed in PBS and incubated with secondary antibodies (Alexa 488 or 546 conjugated, Jackson Laboratories). Nuclei were visualized by DAPI. Sections were analyzed using an Olympus Axioplan2 confocal laser-scanning microscope.

In situ hybridization

In situ hybridization was performed on frozen tissue (tissue preparation as for immunohistochemistry) with digoxigenin (DIG)-labeled riboprobes (Roche) according to standard procedures. Probes were made by cloning of gene-specific PCR products into the StrataClone PCR Cloning Vector using the StrataClone PCR Cloning Kit and subsequent sequencing: *Wnt5a* (1026 bp, nucleotides 629-1635 in NM_009524), *Ttr* (600 bp, 14-614 in NM_013697), *Ngn2* (*Neurog2* – Mouse Genome Informatics) (741 bp, 896-1637 in NM_009718), *Hes5* (1196 bp, 75-1291 in NM_010419).

FACS analysis for cell death (annexin V assay)

E13 hindbrain ChP or cerebral cortices were dissected and dissociated to a single-cell suspension by 15 minute incubation in 0.05% trypsin followed by mechanical dissociation. In cases of co-analysis with prominin 1, the cells were incubated with FITC-conjugated prominin 1 antibody (CD133, eBioscience). Cell death was assessed using the PI/APC-conjugated Annexin V Kit (eBioscience) followed by FACS analysis (FACSAria, BD Biosciences). Gating parameters were determined by side and forward scatter to eliminate debris (P1 gate) and aggregated cells (P2 gate). Non-stained controls were used to set the gates for PI and annexin V (annexin A5 – Mouse Genome Informatics) (set to include no more than 0.1% of non-fluorescent cells). A FITC-conjugated isotype control (eBioscience) was used to set the prominin 1 gate (set to exclude the majority of the cells; see supplementary material Fig. S3). A total of 5000 or 30,000 cells were included in each ChP or cerebral cortex analysis, respectively.

CSF sampling and analysis

Samples of CSF were collected from the fourth ventricle using microcapillary samplers (E12-14, typically 0.5-2 μl) (see Johansson et al., 2006). All CSF samples were microscopically examined for traces of blood over a white background and samples that showed any sign of blood contamination were discarded. The samples were stored at −20°C until analyzed. Total protein concentration was measured using the standard Bradford assay.

Primary cortical cultures

The brains of E13 wild-type embryos were dissected out and the meninges removed. The cerebral cortices were isolated from the rest of the brain and dissociated as previously described (Costa et al., 2008) and cultured in poly-D-lysine-coated 96-well plates (80,000 cells/well) in DMEM-GlutaMAX (Invitrogen) containing CSF (10 or 15%) without further media changes or growth factor additions. After 72 hours the number of cells was assessed using the MTS colorimetric proliferation assay (CellTiter 96 AQueous One Solution Cell Proliferation Assay, Promega). Each sample (n=3 for each condition) contained CSF from six to ten embryos from two to three litters.

Wnt (β-galactosidase) reporter gene assay

Canonical Wnt signaling activity was monitored using the β-Gal Reporter Gene Assay (Roche). Cerebral cortices (pooled from two embryos for each sample) and rostral spinal cords were isolated from E13 *Otx2*$^{fl/fl}$ and *Gdf7-Cre*/*Otx2*$^{fl/fl}$ embryos also carrying the TOPGAL reporter gene (Jackson Laboratories). The chemiluminescence emitted from the deglycosylation of the substrate Galacton Plus was measured using the Orion II Microplate Luminometer (Berthold Detection Systems). Serial dilutions of the β-galactosidase positive control (provided with the kit) were included in the experiments and the concentration of β-galactosidase in each sample was derived from the standard curve.

Transcriptome analysis

Hindbrain ChP was microdissected at E13 from *Gdf7-Cre*/*Otx2*$^{fl/fl}$ and control animals (four pooled samples per genotype, each pooled sample containing two to four ChPs). Total RNA was isolated using the RNeasy Micro Kit (Qiagen) including digestion of remaining genomic DNA. The Agilent 2100 Bioanalyzer was used to assess RNA quality and only high-quality RNA (RIN >8) was used for microarray analysis. Total RNA (80 ng) was amplified using the one-cycle MessageAmp Premier Labeling Kit (Ambion) and 10 μg amplified RNA was hybridized on Affymetrix Mouse Genome 430 2.0 arrays containing ~45,000 probe sets. Staining and scanning were performed according to the Affymetrix expression protocol. Heat maps were generated with CARMAweb and dendrograms with R (hclust) (Rainer et al., 2006). Gene ontology term and pathway enrichment analyses were performed with GePS software (Genomatix, Germany). Secreted proteins were determined with GePS software and manual curation. Array data are available at GEO under accession number GSE27630.

RNA isolation, cDNA synthesis and real-time PCR analysis

Total RNA from microdissected E13 hindbrain ChPs (three to four, pooled), E14-15 lateral ventricular ChPs (one to three, pooled), E13 cerebral cortices (midline excluded, two brains pooled per sample) or E13 rostral spinal cords (two cords pooled per sample) was extracted using the RNeasy Micro Kit (Qiagen) for ChP or the RNeasy Mini Kit (Qiagen) for cortex and spinal cord. RNA was reversed transcribed into cDNA using random primers and Superscript III First-Strand Synthesis SuperMix (Invitrogen). The real-time RT-PCR assay was conducted using SYBR Green Dye Master Mix (Bio-Rad). Primer sets for all genes (supplementary material Table S5) were validated using melting curve analysis and gel electrophoresis. Assays were performed in triplicate on a DNA Engine Opticon machine (Bio-Rad). The relative expression of each mRNA was calculated between the gene of interest and *Gapdh* using the formula $E=2^{-(-\Delta\Delta Ct)}$, and normalized to the expression levels in the control.

Western blot

CSF from E13 *Otx2*$^{fl/fl}$ and *Gdf7-Cre*/*Otx2*$^{fl/fl}$ embryos was sampled as described above. The same volume of CSF was loaded onto each well (12% Tris-HCl gels) and separated by electrophoresis (Mini-PROTEAN 3 Cell System, Bio-Rad). The proteins were transferred onto a PVDF membrane (Millipore) by wet transfer, followed by blocking in Tris-buffered saline containing 5% skimmed milk and then primary antibody incubation in rabbit anti-Tgm2 (1:250, Zedeira) or rabbit anti-Wnt4 (1:500, Abcam), followed by an HRP-conjugated secondary antibody (1:30,000, GE Healthcare). The signal was detected using Immobilon Western Chemiluminescent HRP High-Sensitivity Substrate (Millipore) and X-ray film exposure. Developed X-ray films were digitalized using the CanoScan N670U (Canon) and Adobe Photoshop CS3.

Statistical analysis

Statistical analysis of the microarrays was performed utilizing the statistical programming environment R (R Development Core Team, 2005) implemented in CARMAweb (Rainer et al., 2006). Briefly, probe set summaries were calculated with RMA (R-based Microarray Analysis; default settings including quantile normalization and application of Tukey's median polish algorithm) and genewise testing for differential expression was performed employing the limma *t*-test and Benjamini-Hochberg multiple testing correction [false discovery rate (FDR) <10%].

All other results were analyzed using the unpaired or paired two-tailed Student's *t*-test. The normal distribution of the mutant phenotype was analyzed using the Kolmogorov-Smirnov test for the FACS analysis data (largest dataset) and were found to fit to a normal distribution ($P>0.05$). In all tests, $P<0.05$ was considered statistically significant. All error bars indicate s.e.m.

RESULTS

Otx2 is required for the development of all ChP epithelial cells

In order to study the role of Otx2 in ChP development we generated a new mouse line expressing the tamoxifen-inducible form of Cre (Otx2-CreERT2; supplementary material Fig. S1) in the *Otx2* locus, and mated this with $Otx2^{fl/fl}$ mice in order to conditionally delete *Otx2* upon tamoxifen administration. Tamoxifen (0.1 mg/g body weight) was given to mothers that were pregnant for 9 days, and recombination was monitored in GFP reporter (CAG-GFP) mice (Nakamura et al., 2006). GFP protein was widespread in the dorsal midline at E11 throughout the brain (Fig. 1B,C; supplementary material Fig. S1) and Otx2 protein levels were already reduced in lateral ventricular ChP anlage at E11 (Fig. 1D,E). Transthyretin (*Ttr*) expression was also reduced only 2 days after initiation of recombination at this age (Fig. 1F,G). At E12, the *Ttr*-expressing domain was virtually absent in the rostral part of the lateral ventricular ChP and the third ventricular ChP anlage (Fig. 1H,M). The cortical hem, as visualized by the *Wnt5a*-expressing domain, appeared unaffected at E12, indicating a ChP-specific effect (Fig. 1N,O). Strikingly, at E13, when the lateral and fourth ventricular ChPs are normally both differentiated and invaginated into the ventricle (Fig. 1P,S,U), all four ChPs in the forebrain (including the third ventricular ChP anlage) and hindbrain were virtually absent in the mutant brains (Fig. 1Q,R,T,V; data not shown). In some cases, a small ChP remnant was found caudally, but this was not *Ttr* positive (Fig. 1W,X). Analysis using *Wnt5a*

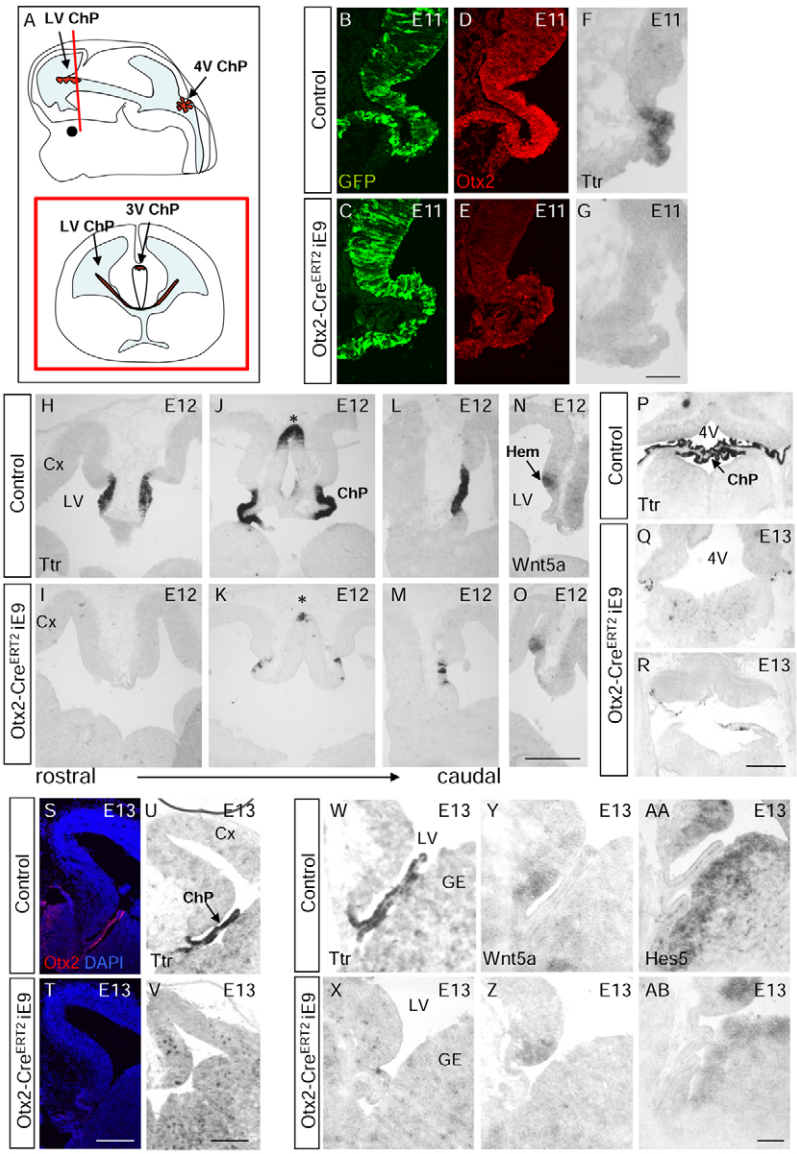

Fig. 1. *Otx2* deletion using Otx2-CreERT2 and E9 induction results in the absence of all four ChPs. (**A**) Schematic showing the localization of all four ChPs in the mouse embryonic brain. The third ventricular ChP is situated between the two lateral ventricular ChPs; they cannot be visualized in the same sagittal representation, and thus a coronal depiction of the forebrain (beneath) shows the localization of the third ventricular ChP and its relation to the two lateral ventricular ChPs. The red line in the sagittal depiction indicates the level of the coronal depiction. (**B-G**) Micrographs of coronal sections of E11 control (*Otx2-CreERT2/CAG-GFP*) and *Otx2-CreERT2/*$Otx2^{fl/fl}$*/CAG-GFP* mice after E9 tamoxifen induction showing recombination in the dorsal midline (B,C; GFP immunohistochemistry) and decrease in Otx2 (D,E; immunohistochemistry) and *Ttr* (F,G; *in situ* hybridization). (**H-O**) Micrographs of coronal sections of E12 control and *Otx2-CreERT2/*$Otx2^{fl/fl}$ mice after E9 tamoxifen induction. *Ttr* (H-M) and *Wnt5a* (N,O) *in situ* hybridization show the virtual absence of all four ChPs but an intact cortical hem territory (M,N). Asterisk indicates the third ventricular ChP. (**P-AB**) Micrographs of coronal sections of E13 control (*Otx2-CreERT2* or $Otx2^{fl/+}$) and *Otx2-CreERT2/*$Otx2^{fl/fl}$ mice after E9-10 tamoxifen induction. (P-R) *Ttr in situ* hybridization shows the absence of the hindbrain ChP after *Otx2* deletion (Q,R). (S,T) Sections stained with an antibody against Otx2. *Ttr in situ* hybridization (U,V) shows the absence of specified ChP territory in rostral sections. *In situ* hybridization for *Ttr* (W,X), *Wnt5a* (Y,Z) and *Hes5* (AA,AB) at more caudal regions of the forebrain show that the former ChP territory remained unspecified. LV, lateral ventricle; 3V, third ventricle; 4V, fourth ventricle; ChP, choroid plexus; Cx, cerebral cortex; GE, ganglionic eminence. Scale bars: 50 μm in B-G; 250 μm in H-O; 100 μm in P-AB.

(Fig. 1Y,Z) and *Hes5* (Fig. 1AA,AB) showed that the hem or neuroepithelial domains were not extended into the ChP domain; instead, a small *Ttr*-negative domain remained at the site of the ChP. Thus, deletion of *Otx2* by Otx2-CreERT2 revealed a key role of Otx2 in the development of all ChPs, resulting in the ultimate disappearance of virtually all ChP cells.

To determine whether Otx2 is also required for the maintenance of the ChP after specification, we induced recombination at E15 in the Otx2-CreERT2 mice (Fig. 2). Five days after induction, Otx2 was no longer detectable in most ChP cells of all four ChPs (Fig. 2A,B; data not shown), with the exception of a very few epithelial cells still being positive (arrow in Fig. 2B); however, the ChP epithelial cells and the entire ChP structures appeared unaltered in size. At 10 days after induction (P7), the size of the lateral and third ventricular ChPs appeared unaffected (Fig. 2C,D; data not shown). However, the fourth ventricular ChP was much smaller (a decrease in rostrocaudal expansion rather than in lateral to medial length; Fig. 2E,F), suggesting a continued, but less acute, role for Otx2 in maintenance of the hindbrain ChP. The reduced size of the fourth ventricular ChP was evident at both medial and lateral levels (sagittal sections) as well as by microscopic inspection of the whole brain. This suggested a region-specific role for Otx2 in ChP maintenance, which is in contrast to the uniform requirement for Otx2 in early ChP development.

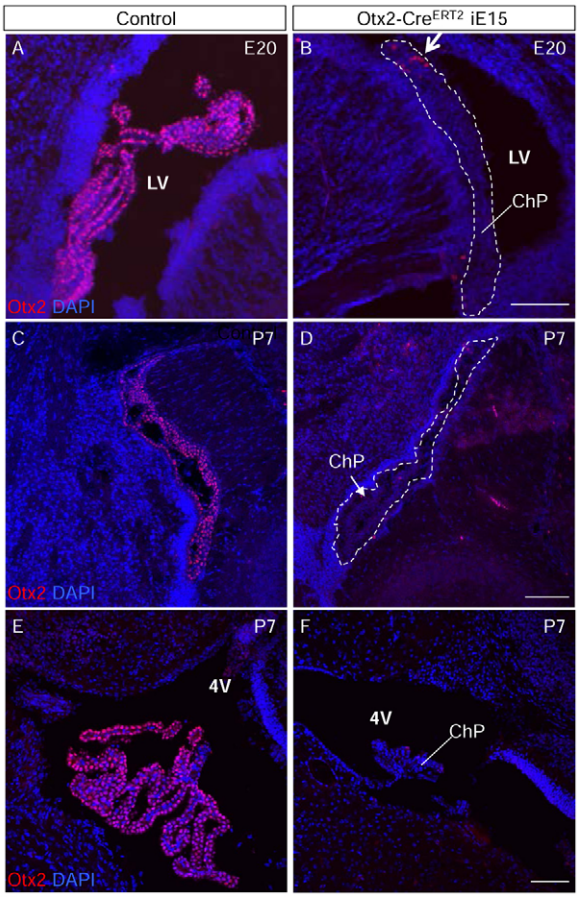

Fig. 2. *Otx2* deletion using Otx2-CreERT2 and E15 induction results in region-specific effects on the ChPs. (**A**,**B**) Confocal images of coronal sections of forebrain immunostained for Otx2 (red) in control and *Otx2-CreERT2/Otx2*$^{fl/fl}$ E20 mice after E15 tamoxifen induction showing the normal appearance of the ChPs despite the absence of Otx2. Note the occasional remaining Otx2^{+} cell (arrow). (**C-F**) Confocal images of sagittal sections immunostained for Otx2 in control and *Otx2-CreERT2/Otx2*$^{fl/fl}$ P7 mice after E15 tamoxifen induction showing normal sized lateral ChPs (D, outlined with dashed lines) but a smaller hindbrain ChP (F). LV, lateral ventricle; 4V, fourth ventricle. Scale bars: 100 μm.

Otx2 is required for the survival of cells in the hindbrain ChP

Although the above data suggest a key role of Otx2 in ChP development, CreERT2-mediated deletion is not specific to the roof plate and ChP regions, but also occurs in the ventral telencephalon, midbrain and various other regions of the brain expressing Otx2 (supplementary material Fig. S1). We therefore searched for a more ChP-specific Cre driver. As recombination in the Gdf7-Cre mouse line has previously been shown to be specific to the roof plate and to occur in the cells generating the hindbrain ChP (Lee et al., 2000; Currle et al., 2005), we examined Gdf7-Cre-mediated recombination in the *Otx2*$^{fl/+}$ background. We observed recombination in the hindbrain ChP, in the dorsal midline of the midbrain and the diencephalon (supplementary material Fig. S2), and very little recombination in the lateral ventricular ChP (in only a few cells in a restricted number of sections of the ChP; supplementary material Fig. S2). We also saw reporter gene expression in what appeared to be the telencephalic meninges, as well as in scattered cells in the hind- and midbrain areas (supplementary material Fig S2).

Consistent with the virtual absence of recombination in the lateral ventricular ChPs, all DAPI-labeled epithelial cells were still Otx2 immunopositive from E13 to E16 (Fig. 3A-D), the *Otx2* mRNA levels were comparable (Fig. 3E) and no significant defects in size or maturation of the lateral ventricular ChPs in *Gdf7-Cre*/*Otx2*$^{fl/fl}$ mice or controls (*Gdf7-Cre*/*Otx2*$^{fl/+}$ or *Otx2*$^{fl/fl}$) were detectable (Fig. 3F-J). The nearby cortical hem also appeared normal (Fig. 3K,L). Likewise, the third ventricular ChP also appeared normal (Fig. 3G-J) despite higher levels of reporter gene activity in this region (supplementary material Fig. S2). Conversely, we observed a dramatic decrease in the size of the hindbrain ChP by E13 (Fig. 4C,D), but not yet consistently so at E12 (Fig. 4A,B). The reduction in size was seen in all *Gdf7-Cre*/*Otx2*$^{fl/fl}$ embryos in all coronal sections containing hindbrain ChP, and was not due to Cre toxicity as the heterozygous embryos (*Gdf7-Cre*/*Otx2*$^{fl/+}$) did not exhibit this phenotype. Accordingly, *Otx2* mRNA levels as measured by real-time RT-PCR were significantly decreased in hindbrain ChP tissue isolated from E13 *Gdf7-Cre*/*Otx2*$^{fl/fl}$ versus control embryos (Fig. 4E).

Analysis of serial sections of the ChP revealed that the recombination efficiency was not complete at all levels, as visualized by the absence of GFP reporter in some fourth ventricular ChP epithelial cells (Fig. 4F; compare also with supplementary material Fig. S2L). Notably, many of the ChP cells remaining at E13 (Fig. 4G) were not reporter positive, suggesting that some epithelial cells escape the *Otx2* deletion and thus the E13 ChPs in *Otx2*$^{fl/fl}$ mice mostly consist of non-recombined Otx2^{+} cells. The concept of 'escaping' epithelial cells was verified by the presence of a smaller Otx2^{+} hindbrain ChP remaining at lateral levels at P2 (Fig. 4H,I) and in the adult (data not shown). The presence of a much smaller ChP at P2 and adult stages also indicated the absence of compensatory growth or regrowth of the ChP. Thus, Gdf7-Cre-mediated *Otx2* deletion results in a significant reduction in the size of the hindbrain ChP, while not evidently affecting the ChP of the lateral and third ventricles.

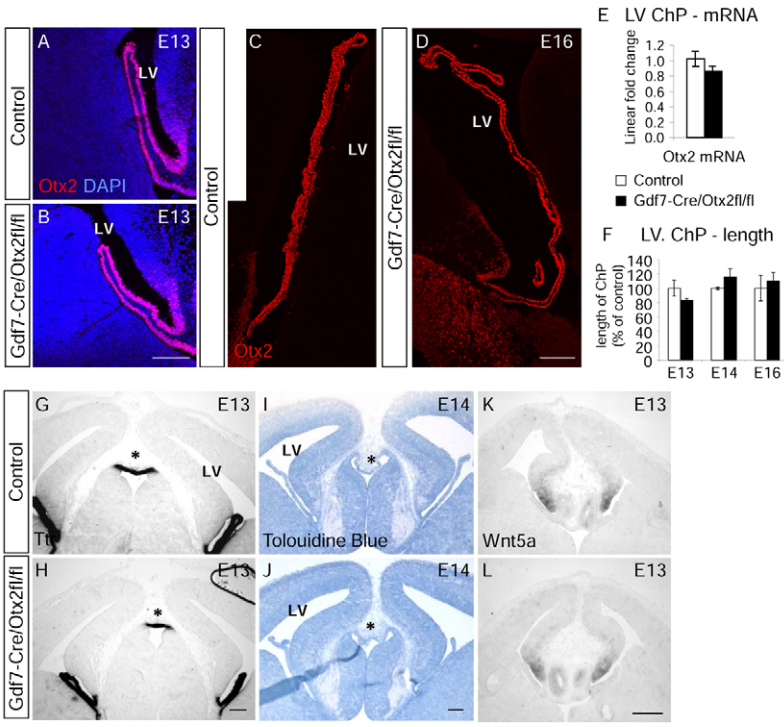

Fig. 3. The forebrain ChPs remain unaffected in *Gdf7-Cre/Otx2*$^{fl/fl}$ mice. (**A-D**) Confocal image stacks of coronal sections of forebrain ChP from E13 (A,B) and E16 (C,D) control and *Gdf7-Cre/Otx2*$^{fl/fl}$ embryos immunostained for Otx2 (red), with nuclei labeled with DAPI (blue). (**E**) Relative *Otx2* mRNA levels in isolated E14/15 lateral ventricular ChP. (**F**) Relative length of the lateral ventricular ChP at E13-16. Error bars indicate s.e.m. (**G-L**) Micrographs showing *Ttr in situ* hybridization (G,H), Tolouidine Blue staining (I,J) and Wnt5a *in situ* hybridization (K,L) in coronal sections of forebrain ChPs from E13 control and *Gdf7-Cre/Otx2*$^{fl/fl}$ embryos. Asterisk indicates the third ventricular ChP. LV, lateral ventricle. Scale bars: 100 μm.

To evaluate the possibility of increased cell death as a cause for the size reduction observed in the *Gdf7-Cre/Otx2*$^{fl/fl}$ hindbrain ChP, we used fluorescence-activated cell sorting (FACS) of annexin V and propidium iodide (PI) (Fig. 5A,B; supplementary material Fig. S3). This revealed a significant increase in both late (PI$^+$/annexin V$^+$, 2.4-fold increase) and early (annexin V$^+$, 2.1-fold increase) apoptosis among cells isolated from the E13 *Gdf7-Cre/Otx2*$^{fl/fl}$ hindbrain ChP compared with controls (Fig. 5B). The percentage of necrotic cells (PI only; Fig. 5B) was low in all samples and not significantly altered in the mutant. To assess the levels of apoptosis specifically in the ChP epithelial cells, we used double labeling with an antibody recognizing prominin 1 (CD133) localized on the ChP epithelial cells (Fig. 5C). As expected, prominin 1$^+$ epithelial cells from the mutant *Gdf7-Cre/Otx2*$^{fl/fl}$ ChP showed an increase in apoptosis (late and early apoptosis combined, 2.5-fold increase; Fig. 5D), suggesting that ChP epithelial cells enter the apoptosis pathway upon deletion of *Otx2*.

The reduced ChP size and increased cell death might be due to aberrant proliferation. Staining for the phosphorylated form of histone H3 (PH3) that is present in late G2/M phase of the cell cycle revealed a significant reduction of PH3$^+$ cells in the hindbrain ChP of *Gdf7-Cre/Otx2*$^{fl/fl}$ compared with control embryos [Fig. 5E-G; the proliferative zone belonging to the ChP is delineated by the absence of Pax6 (Landsberg et al., 2005)], suggesting that reduced proliferation might further contribute to the decreased size of the *Gdf7-Cre/Otx2*$^{fl/fl}$ hindbrain ChP at this age.

Given the signaling between the ChP epithelial and endothelial cells (Wilting and Christ, 1989; Nielsen and Dymecki, 2010), we also examined blood vessels by PECAM immunohistochemistry. The blood vessels formed at normal density in the *Gdf7-Cre/Otx2*$^{fl/fl}$ hindbrain ChP region, even though they appeared somewhat more disorganized (supplementary material Fig. S3). Thus, various defects occur after Otx2 protein loss at ~E13 in the hindbrain ChP, the most prominent of which is pronounced cell death.

Changes in CSF composition after deletion of *Otx2* in the hindbrain ChP

As the hindbrain ChP develops first and is the largest at E13, we hypothesized that its severe reduction might affect CSF composition. Total protein concentration was determined in CSF collected from control and *Gdf7-Cre/Otx2*$^{fl/fl}$ embryos using the standard Bradford assay. This analysis revealed a significant increase in CSF protein concentration in the *Gdf7-Cre/Otx2*$^{fl/fl}$ mice at E13 and E14 (30% and 60% increases over control values, respectively) but not at E12 (Fig. 6A).

In order to assess whether the altered composition of CSF from mutant embryos had any functional consequences (and to examine the extent to which an *in vivo* phenotype could be due purely to altered intraventricular pressure resulting from the smaller ChP), CSF from control and *Gdf7-Cre/Otx2*$^{fl/fl}$ mice was sampled from the fourth ventricle (E13) and added to primary dissociated cerebral cortex cultures from E13 wild-type mice (Costa et al., 2008). The cells were grown for 3 days in DMEM-GlutaMAX and 10% CSF from either genotype (with no additional growth factors or mitogens). Interestingly, the number of cells, as shown by the MTS assay, was significantly increased when CSF from *Gdf7-Cre/Otx2*$^{fl/fl}$ mice was added as compared with CSF from control mice (35% increase; Fig. 6B). This was not due to a global increase in CSF protein, as the addition of more control CSF (15%) did not alter cell numbers. Thus, depletion of hindbrain ChP by Gdf7-Cre-mediated *Otx2* deletion affects CSF composition.

Transcriptome analysis of hindbrain ChP reveals major alterations in the expression of secreted signaling factors in *Gdf7-Cre/Otx2*$^{fl/fl}$ embryos

Given the above results we next set out to determine the factors that are altered in the *Gdf7-Cre/Otx2*$^{fl/fl}$ CSF, supposedly based on altered expression/release from the hindbrain ChP. Genome-wide expression analysis of microdissected control (*Otx2*$^{fl/fl}$) and mutant hindbrain ChP was performed using Affymetrix MOE430 2.0

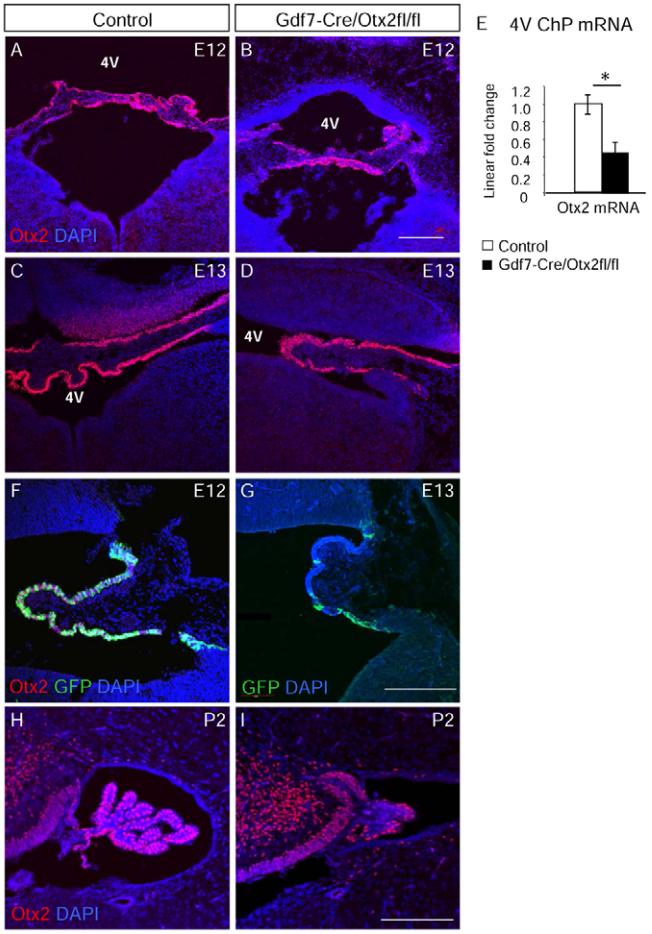

Fig. 4. *Otx2* deletion using the Gdf7-Cre mouse line results in a smaller hindbrain ChP. (**A-D**) Confocal image stacks of coronal sections of the hindbrain ChP from E12-13 control and *Gdf7-Cre/Otx2*$^{fl/fl}$ mice immunostained for Otx2 (red). (**E**) Relative *Otx2* mRNA levels in isolated E13 hindbrain ChP. *P<0.05; error bars indicate s.e.m. (**F**,**G**) Confocal image stacks of coronal sections of the hindbrain ChP from P2 control and *Gdf7-Cre/Otx2*$^{fl/fl}$ mice immunostained for Otx2 and GFP. (**H**,**I**) Confocal image stacks of coronal sections of the hindbrain ChP from *Gdf7-Cre/CAG-GFP* and *Gdf7-Cre/Otx2*$^{fl/fl}$*/CAG-GFP* mice immunostained for Otx2 and GFP. 4V, fourth ventricle. Scale bars: 200 μm.

arrays. Clustering of the array data (supplementary material Fig. S4) grouped the samples according to their genotype. Reassuringly, genes already known to be highly expressed in the ChP, such as the very abundant *Ttr*, Igf and *Aqp1* mRNAs (Lehtinen et al., 2011; Marques et al., 2011), were also highly expressed in the current analysis. Indeed, *Ttr* is the second most abundant mRNA in E13 control ChP and is similarly abundant in the mutant ChP, suggesting that our dissection procedure was successful in isolating the remnant ChP and that no major change in composition of the ChP was evident.

The transcriptome analysis revealed 511 significantly (FDR<10%) differentially expressed probe sets, which had expression levels exceeding 50 in at least one group and linear ratios that exceeded 2-fold (supplementary material Fig. S4). In total, 192 probe sets were upregulated (corresponding to 135 genes) and 319 downregulated (corresponding to 225 genes) (supplementary material Tables S1, S2). In order to validate the differences in gene expression as predicted by the microarray analysis, ten genes (chosen for their biological significance as well as to represent a range of fold changes and expression levels) were investigated by real-time RT-PCR (on the same RNA used for the arrays as well as on independent samples). The up- or downregulation of all selected genes was confirmed, and nine out of ten RT-PCR results were significant (P<0.05; supplementary material Fig. S4).

We then focused specifically on genes encoding diffusible factors (supplementary material Tables S3, S4) and noted several components of the Wnt signaling pathway with significantly altered expression in the *Gdf7-Cre/Otx2*$^{fl/fl}$ hindbrain ChP (Table 1). The upregulation of *Rspo1*, *Wnt4*, *Sfrp2* and *Tgm2*, as well as the downregulation of *Sostdc1*, would all point to increased Wnt signaling mediated via the CSF. Conversely, no changes were observed in the expression of Igf and related factors previously suggested to play important roles in signaling via the CSF (Huang et al., 2010; Lehtinen et al., 2011).

In order to directly measure some of the Wnt signaling modulators that display altered expression in the mutant hindbrain ChP, CSF was sampled from several embryos, pooled as one biological replicate and equal volumes of control and mutant CSF were loaded onto single lanes on a western blot (n=3 biological replicates). Remarkably, Wnt4 and Tgm2 were not only detectable in the CSF collected from control embryos (Fig. 6C), but both also showed a considerable increase in concentration in the CSF from *Gdf7-Cre/Otx2*$^{fl/fl}$ embryos (Fig. 6C), thereby confirming that the gene expression changes observed in the mutant hindbrain ChP are reflected at the protein level in the CSF.

Altered proliferation and Wnt signaling in the cerebral cortex

As the above data suggest that the deletion of the *Otx2*$^{-/-}$ hindbrain ChP affects CSF composition, including modulators of the Wnt pathway, we examined the extent to which this affects the neuroepithelial cells lining the ventricle. As Wnt signaling would affect proliferation, we examined PH3 in three different regions of the *Gdf7-Cre/Otx2*$^{fl/fl}$ mice, namely the cerebral cortex, the lateral ganglionic eminence (LGE) and the spinal cord, all of which are in contact with CSF. Even though Gdf7-Cre-driven recombination did not affect the forebrain (see also supplementary material Fig. S2), we found an increase in apical (ventricle-contacting) PH3$^+$ cells per hemisphere (30% increase; Fig. 7A-C; see also supplementary material Fig. S5), whereas PH3$^+$ basal progenitors were slightly reduced (by 10%) in number (Fig. 7A-C) in the cerebral cortex of *Gdf7-Cre/Otx2*$^{fl/fl}$ E13 embryos. These data are consistent with the role of Wnt signaling in promoting stem cell self-renewal, causing a decrease in the generation of intermediate neuronal progenitors dividing basally. This effect appeared to be surprisingly specific to the dorsal telencephalon as no changes in proliferation were observed in either the LGE of the ventral telencephalon or in the spinal cord (Fig. 7D,E; supplementary material Fig. S5).

As the smaller hindbrain ChP was primarily caused by an increase in apoptosis, and as diffusible and secreted factors regulating apoptosis could reach the cerebral cortex via the CSF, we also investigated cell death in the cerebral cortex at E13 by FACS analysis of annexin V as described above (Fig. 7F). No changes in apoptosis were seen in the radial glia (prominin 1$^+$ cells), whereas a decrease (by 25%) in apoptosis was seen in the prominin 1$^-$ population (basal progenitors and neurons). This decrease could potentially explain the decrease in PH3$^+$ basal progenitors, but not the increase in PH3$^+$ apical progenitors, consistent with the increase in apical progenitors being caused by increased Wnt signaling from the CSF.

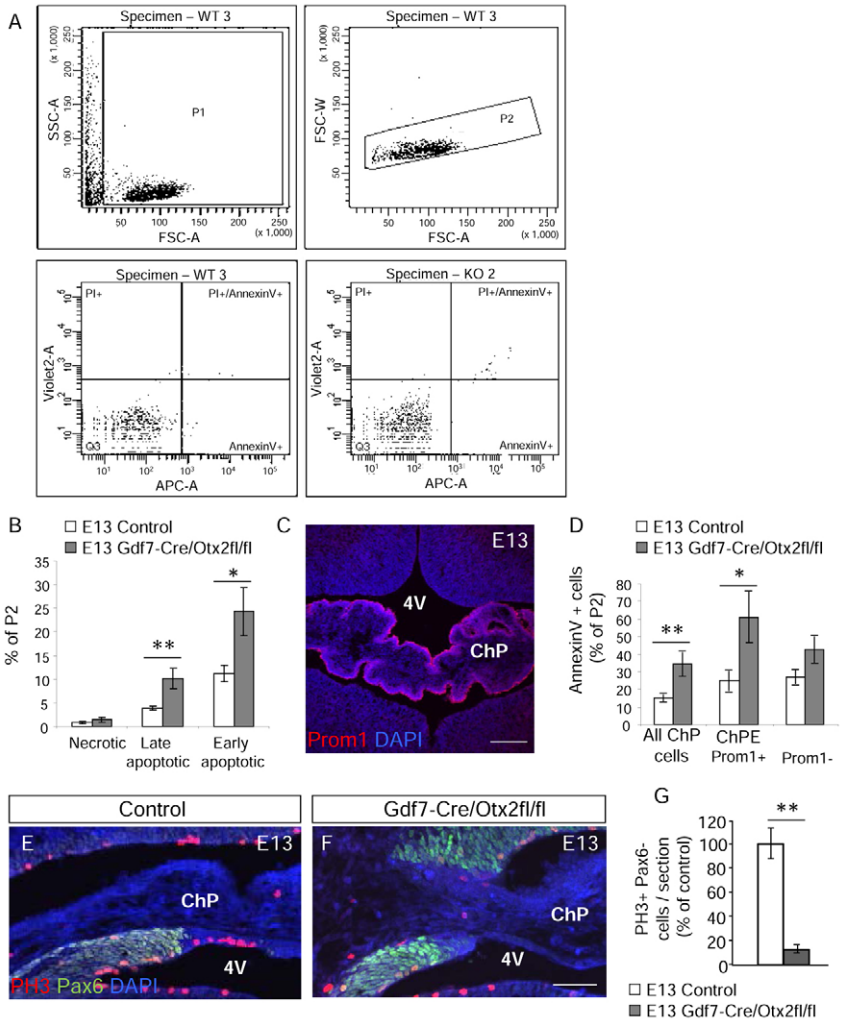

Fig. 5. The reduced size of the hindbrain ChP after *Otx2* deletion using the Gdf7-Cre mouse line results mainly from an increase in apoptosis. (**A**) FACS setup showing P1 and P2 gates (far left and left) and the selection of cells for analysis and example blots (right and far right) from one control (WT 3) and one mutant (KO 2) analysis. (**B**) Quantification of the FACS analysis. (**C**) Micrograph depicting prominin 1 immunostaining in the epithelial cells of control hindbrain ChP at E13. Nuclei are labeled with DAPI. (**D**) Quantification of the prominin 1 co-analysis; n=6-8. (**E**,**F**) Micrographs of coronal sections depicting proliferating cells of the hindbrain ChP labeled by phospho-histone H3 (PH3) antibody and absence of Pax6. (**G**) Quantification of $PH3^+$ cells in the hindbrain ChP; n=3. *P<0.05, **P<0.01; error bars indicate s.e.m. ChPE, ChP epithelial cells; 4V, fourth ventricle. Scale bars: 100 µm in C; 40 µm in E,F.

To determine which signaling pathways might be involved in the alterations in proliferation, we used real-time RT-PCR to determine the expression of genes considered to be direct target genes of particular signaling pathways. This analysis, of RNA isolated from the cerebral cortices, revealed significant changes in the expression of target genes associated with Wnt signaling and proliferation (cyclin D1, upregulated) as well as the Notch signaling pathway (*Hes1* and *Ngn2*, downregulated), but no changes in target genes associated with the Shh, Fgf or Tgfβ signaling pathways (supplementary material Fig. S6).

To directly monitor canonical Wnt signaling in tissues in contact with the altered CSF, we crossed *Gdf7-Cre*/*Otx2*$^{fl/fl}$ mice with the TOPGAL (TG) reporter mice carrying a β-galactosidase reporter driven by several TCF/Lef binding sites (DasGupta and Fuchs, 1999). We then investigated whether Wnt reporter localization (Fig. 7G,H) or levels (Fig. 7I) were altered in the embryos with a mutant hindbrain ChP. The localization of β-galactosidase (as visualized by immunohistochemistry) was unchanged in the *Gdf7-Cre*/*Otx2*$^{fl/fl}$/*TG* mice, with no apparent ectopic Wnt activity in the neuronal population, nor was there a spreading of the hippocampal anlage into the cortex proper, suggesting no change in this aspect of neocortical patterning. However, quantification of the levels of β-galactosidase using a chemiluminescent assay revealed a significant increase (by 30%; Fig. 7I) in E13 cerebral cortices from mutant (*Gdf7-Cre*/*Otx2*$^{fl/fl}$/*TG*) compared with control (*Otx2*$^{fl/fl}$/*TG*) mice, with no significant changes in the spinal cord (data not shown). Thus, region-specific alterations in canonical Wnt signaling correspond to the region-specific changes in proliferation and modulation of Wnt signaling components in the CSF.

Long-term effects of transient alterations in cortical Wnt signaling

Next, we investigated how the alterations in the cerebral cortex would further develop. Interestingly, the increase in proliferation observed at E13 had reversed at E16, when we found a decrease in $PH3^+$ cells at the apical surface (40% decrease; Fig. 8A). This alteration in the proliferation phenotype could be explained by an intrinsic compensatory effect in the progenitor cells with regard to proliferation and/or apoptosis (e.g. Ciaroni et al., 1995), by differences in Wnt signaling (levels and response) at later stages of embryonic development (Chenn, 2008; Pöschl et al., 2012), or could be due to the alterations in CSF composition, which are now greatly modulated by the large and phenotypically normal lateral ventricular ChP reducing the influence of the hindbrain ChP. In accordance with the two latter options, the increased levels of Wnt signaling found at E13 were no longer detectable at E16 (Fig. 8B), suggesting that the changes seen earlier were transient.

We then investigated the long-term effects of this transient increase in Wnt signaling by immunohistochemical analysis of the cerebral cortex at P7 (Fig. 8C). Although no gross defects were

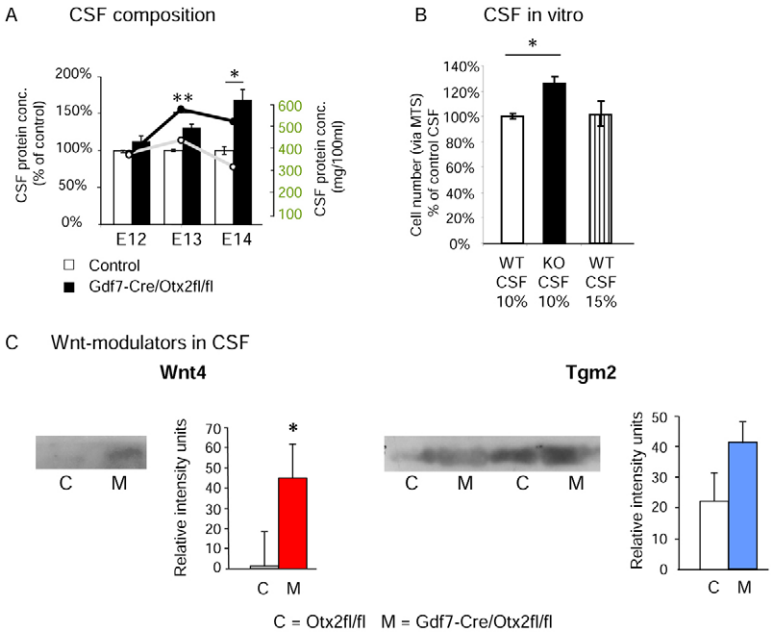

Fig. 6. The smaller hindbrain ChP after *Otx2* deletion using the Gdf7-Cre mouse line alters CSF composition. (**A**) Relative and total protein concentrations in CSF sampled from the fourth ventricle. A significant increase in protein levels was seen in CSF from *Gdf7-Cre/Otx2*$^{fl/fl}$ mice at E13 and E14; *n*=4-6. (**B**) An increase in the number of cortical cells after 3 days in culture with media supplemented with CSF from E13 *Gdf7-Cre/Otx2*$^{fl/fl}$ versus control embryos; *n*=3. (**C**) Western blot analysis of Wnt4 and Tgm2 concentration in CSF from E13 control and *Gdf7-Cre/Otx2*$^{fl/fl}$ embryos. Equal volumes of CSF were loaded onto the gel and their relative concentration analyzed, showing increased concentrations of both Wnt4 and Tgm2 in CSF from the mutant embryos. **P*<0.05, ***P*<0.01; for the Tgm2 analysis *P*=0.09; error bars indicate s.e.m.

detected at this stage, histological analysis revealed a region-specific reduction (by 20%) in layer 5 neurons (detected as Ctip2^{+}/Tbr1^{-} cells; Fig. 8D-I). As these neurons are largely produced at the time when we observe an increase in proliferation, this phenotype is consistent with the progenitor cells remaining longer in the cell cycle rather than exiting to differentiate into neurons. Conversely, layers containing neurons generated earlier or later were not significantly altered in their thickness.

DISCUSSION

Otx2 as a master regulator of ChP development and maintenance

Here we demonstrated a key role for Otx2 in ChP development by deletion of *Otx2* at three different time points during development using two distinct Cre lines. Deletion of *Otx2* during the initial stages of development affects ChP development rapidly and profoundly. Upon deletion of *Otx2* by induction of recombination at E9 and complete absence of Otx2-immunopositive cells by E11, all ChPs failed to form. Notably, this was a ChP-specific effect, as another roof plate-derived structure that also expresses Otx2, the nearby cortical hem, was unaffected. Thus, whereas Otx2 is not vital for the hem, it is absolutely required for all four ChPs, with very little remnant structures at E12/13 in the absence of Otx2. The vast majority of ChP cells are either not specified or die at such an early state in their differentiation that they cannot be distinguished. Notably, a very small remnant structure (estimated at 1-2% of control ChP size) of the lateral ChP remains as a single layer of non-pseudostratified epithelium that is clearly distinct from the adjacent neuroepithelium but still largely fails to differentiate ChP hallmarks such as Ttr expression.

A similarly profound role for Otx2 was seen at later stages when using the Gdf7-Cre driver (onset of protein loss at E11/12), with only Otx2^{+} cells – either escapers from recombination (GFP reporter negative/Otx2^{+}) or in the process of losing Otx2 (GFP^{+}/Otx2^{+}; reduced *Otx2* mRNA levels at E13 suggest ongoing loss of Otx2) – surviving and forming the ChP remnants. When Otx2 protein is lost at these slightly later stages ChP cells still succumb immediately to cell death, as they are unable to survive without sufficient levels of Otx2.

These data revealed Otx2 as a master regulator of ChP development, it being absolutely essential for these structures to appear. Strikingly, this essential role remains when Otx2 protein is deleted at E20 and the hindbrain ChP subsequently decreases significantly in size. As less proliferation occurs at this time, this effect is also likely to be due to many ChP cells undergoing cell death. Interestingly, in other systems loss of Otx2 also leads to an increase in apoptosis, such as in the adult mouse retinal pigment epithelium and photoreceptors and in GnRH neurons (Béby et al., 2010; Diaczok et al., 2011). These results imply a role for Otx2 as a key regulator of genes that are essential for the function and identity of these cells, such that they fail to survive without them, or the direct regulation by Otx2 of anti-apoptotic genes. The latter function has recently been demonstrated for a variety of homeobox and paired-type homeobox transcription factors (Ninkovic et al., 2010; Fuchs et al., 2012; Moon et al., 2012).

A further exciting and entirely unexpected result is the region-specific effect of Otx2 in ChP maintenance, as observed upon Otx2-CreERT2 line induction at E15. Whereas the hindbrain ChP was severely reduced in size by P7, this was not obvious for the other ChPs, suggesting – to our knowledge for the first time – region-

Table 1. Microarray data for genes with significantly altered expression in *Gdf7-Cre/Otx2*$^{fl/fl}$ hindbrain ChP that encode diffusible components of Wnt signaling

Gene	Ratio*	KO‡	WT‡	Documented effect on Wnt signaling
Wif1	2.6	312	118	Decrease
Rspo1	3.0	481	161	Increase
Wnt4	2.1	737	356	Increase
Sfrp2	2.1	1420	692	Decrease or increase
Dkk2	6.9	2214	322	Decrease or increase
Tgm2	2.0	480	236	Increase
Sostdc1 (*Wise*)	0.4	1808	4209	Decrease

*Linear ratio of *Otx2* knockout/control.
‡Average expression level in *Otx2* knockout (KO) or wild type (WT).

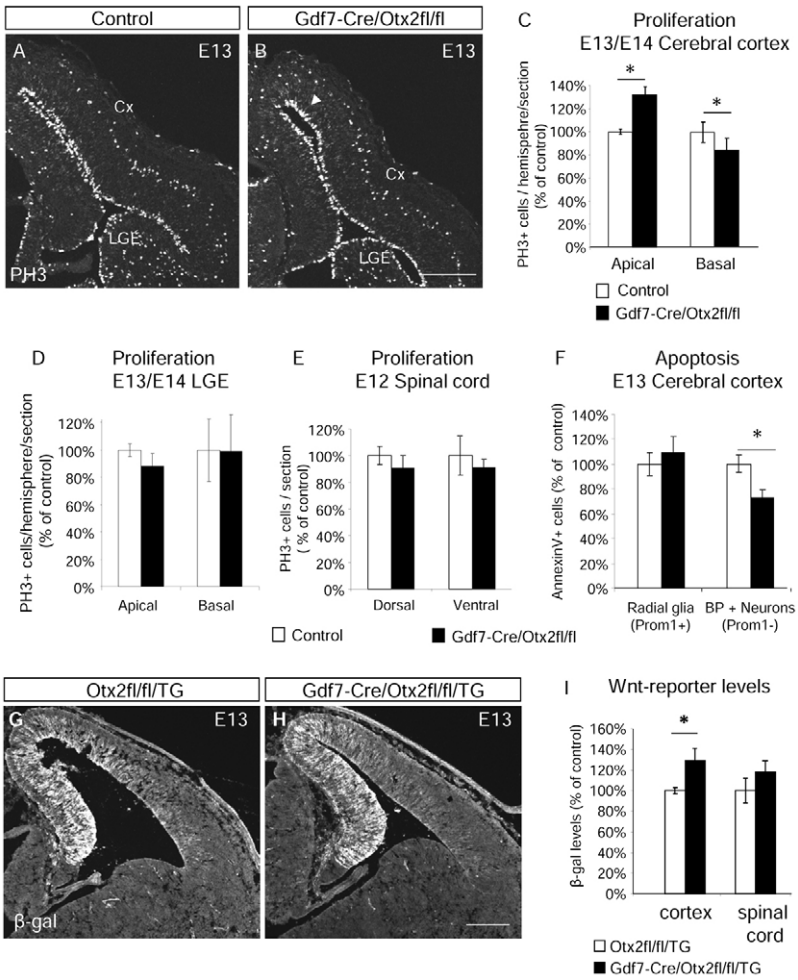

Fig. 7. Changes in cerebral cortex proliferation and Wnt signaling after deletion of *Otx2* in the hindbrain ChP using Gdf7-Cre. (**A**,**B**) Micrographs of coronal sections of forebrain immunostained for PH3. Note the increase in the number of apically proliferating cells in the cerebral cortex (Cx) (arrowhead) in the *Gdf7-Cre/Otx2*$^{fl/fl}$ mice. (**C-E**) Quantification of PH3^{+} cells in cortex (C), lateral ganglionic eminence (LGE) (D) and spinal cord (E). PH3 quantifications showed a significant increase in apically dividing cells in the cerebral cortex and a significant decrease in basally dividing cells at E13/E14. *n*=5. (**F**) Levels of apoptosis (FACS analysis of annexin V) in E13 cerebral cortex showing no change in radial glia (prominin 1^{+} cells) but a small decrease in apoptosis in prominin 1^{-} cells [basal progenitors (BP) and neurons]. *n*=5. (**G**,**H**) Micrographs of coronal sections of forebrain from control (*Otx2*$^{fl/fl}$*/TG*; C) and *Gdf7-Cre/Otx2*$^{fl/fl}$*/TG* (D) embryos immunostained for β-galactosidase. No change in the localization of the Wnt reporter was observed. (**I**) Quantification of Wnt signaling in control (*Otx2*$^{fl/fl}$*/TG*) and *Gdf7-Cre/Otx2*$^{fl/fl}$*/TG* cortices and spinal cords, showing a significant increase in Wnt signaling in the cerebral cortices from embryos with a mutant hindbrain ChP. *n*=5. *P<0.05; error bars indicate s.e.m. Scale bars: 200 μm.

specific differences between the ChPs at this stage. It is now of importance to unravel the region-specific differences in ChPs at the molecular and cellular levels. In this regard, it is of interest that we detected an increase in Wnt signaling components and modulators in the CSF when the hindbrain ChP was most affected by earlier *Otx2* deletion, whereas other signaling molecules in the CSF, such as Shh (Huang et al., 2010) and Igf (Lehtinen et al., 2011), were not altered in their expression levels in the mutant hindbrain ChP. Thus, our work revealing the key role of Otx2 in ChP development now opens novel avenues to further our understanding of these key structures in the developing brain.

Wnt-mediated signaling via the CSF

In addition to revealing Otx2 as a novel key regulator of ChP development, our data are also consistent with a new role for the hindbrain ChP in long-distance signaling mediated by members and modulators of the Wnt signaling pathway (see supplementary material Fig. S7). In the present study, we found that Gdf7-Cre-mediated deletion of *Otx2* leads to changes in CSF composition that affect the proliferation of cells from the cerebral cortex *in vitro* and *in vivo*. CSF sampled from *Gdf7-Cre*/*Otx2*$^{fl/fl}$ mice and administered to cell cultures of cerebral cortex progenitors resulted in increased cell numbers, consistent with the increased proliferation of cells in this region of the mutant embryos. Moreover, based on a transcriptome analysis of the mutant hindbrain ChP that revealed increased expression of Wnt4 and Tgm2, a positive modulator of Wnt signaling (Beazley et al., 2012), we also detected increased levels of these proteins in the CSF of *Gdf7-Cre*/*Otx2*$^{fl/fl}$ mice compared with that collected from control littermates. We then showed that the activity of a TCF/Lef reporter is increased in the cerebral cortex, but not the spinal cord, in the mutant mice, consistent with increased proliferation in the region with increased levels of Wnt signaling. Moreover, the region-specific effects demonstrate that despite the ubiquitous contact of neuroepithelial cells with the CSF, their intrinsic competence regulates their response, as cells in the LGE and spinal cord did not exhibit altered proliferation or Wnt signaling. Thus, our work unraveled a novel route of Wnt signaling from the hindbrain ChP via the CSF.

Interestingly, Otx2 has previously been shown to regulate Wnt ligands, directly or indirectly, along with other signaling molecules in various tissues during development; for example, Wnt ligands and Nodal in the anterior visceral endoderm (Perea-Gomez et al., 2001) and Wnt1, Fgf8 and Shh in the mid/hindbrain region (Acampora et al., 1997; Puelles et al., 2003; Prakash et al., 2006; Omodei et al., 2008). These data prompt the suggestion that Otx2 might commonly affect targets of the Wnt pathway in various cell types, with distinct effects depending on the region and developmental stage. Moreover, Otx2-deficient hindbrain ChP was also altered in the expression of other diffusible signaling molecules, such as members and modulators of the Fgf and Tgfβ families, supporting Otx2 as a key regulator of non-cell-autonomous signaling in development.

However, it is important to bear in mind that the gene expression changes observed in our study might not be solely due to a direct

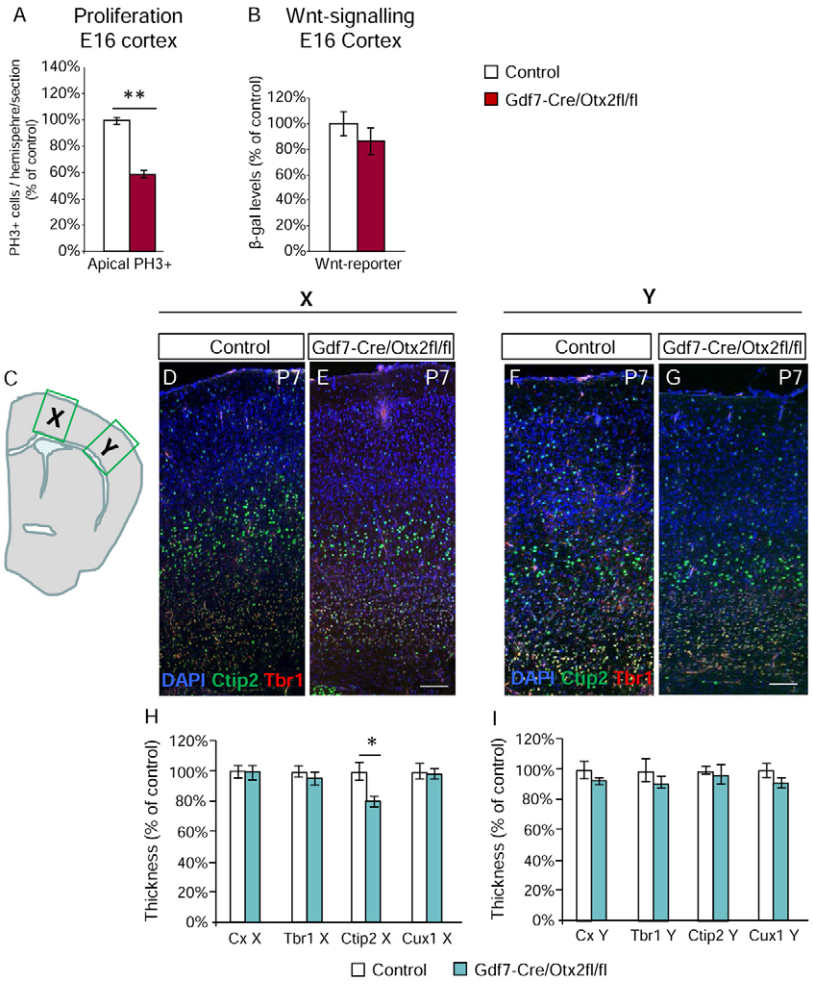

Fig. 8. Changes in mouse cerebral cortex development at E16 and P7 after deletion of *Otx2* in the hindbrain ChP using Gdf7-Cre. (**A**,**B**) Quantification of the percentage of apical PH3$^+$ cells (A) and β-galactosidase levels (B) in E16 control and *Gdf7-Cre/Otx2*$^{fl/fl}$ cortices, showing a decrease in proliferation. *n*=3-5. (C-I) P7 analysis. (**C**) Schematic of the approximate rostrocaudal level and areas (X and Y) analyzed. (**D-G**) Micrographs of coronal sections of forebrain immunostained for Tbr1 and Ctip2 from control (*Otx2*$^{fl/fl}$; D,F) and *Gdf7-Cre/Otx2*$^{fl/fl}$ (E,G) pups. (**H**,**I**) Quantification of cortical and cortical layer thickness in area X (H) and Y (I). *n*=4-5. **P*<0.05, ***P*<0.01; error bars indicate s.e.m. Scale bars: 100 μm.

effect of Otx2 loss, as a change in composition of the ChP itself (e.g. the ratio of epithelial cells to stroma) and other secondary effects due to the induction of apoptosis might well contribute to changes in expression levels. Notably, the Otx2 protein itself is also secreted (Sugiyama et al., 2008) and might hence be present in different amounts in the CSF from *Gdf7-Cre/Otx2*$^{fl/fl}$ embryos compared with control embryos. However, no Otx2 protein was detectable in the ventricular zone of the cerebral cortex, which does not express *Otx2* mRNA, suggesting that the amount of Otx2 protein taken up by these cells is, if at all, rather low under control conditions.

Interestingly, the changes in CSF composition in the *Gdf7-Cre/Otx2*$^{fl/fl}$ embryos appear to be largely mediated by the defects in the hindbrain ChP, as no defects were detectable in the ChPs of the lateral and third ventricle. This would suggest that most, if not all, of the phenotypic abnormalities observed in the cerebral cortex (increased Wnt signaling and proliferation) should be caused by impaired development and functioning of the hindbrain ChP. This hypothesis is further supported experimentally by the observation that CSF sampled from the fourth ventricle of *Gdf7-Cre/Otx2*$^{fl/fl}$ mutant mice affects cerebral cortex progenitors *in vitro* in a way that strongly resembles the phenotype observed *in vivo*. Moreover, changes in mRNA levels in the hindbrain ChP and in the CSF concentration of positive Wnt regulators fit with a major role of the hindbrain ChP in mediating these changes.

However, we noted that recombination mediated via Gdf7-Cre also occurs in the midbrain roof plate, which expresses Otx2 and is in contact with the CSF, suggesting that these cells might contribute to the observed changes in CSF composition, even if they are not visibly defective in their development. Also, if other regions contribute to this phenotype, this work highlights the key roles of ChP differentiation in signaling during brain development beyond neighboring regions (Huang et al., 2010). Given the profoundly altered expression levels of Wnt4 and other modulators of Wnt signaling in the hindbrain ChP upon Gdf7-Cre-mediated *Otx2* deletion, we suggest that this ChP at least contributes to the alterations in Wnt signaling in the distant cerebral cortex via changes in CSF composition. This supports the hypothesis of a modulatory fine-tuning effect mediated by the CSF.

Consistent with the modest change in Wnt signaling and proliferation (with regard to both timing and magnitude) we detected a small region- and layer-specific change in neuronal number as a consequence of manipulation of the hindbrain ChP. Interestingly, changes in neuron numbers in specific layers of the cerebral cortex occur in a region-specific manner during phylogeny and ontogeny, in order to achieve the area-specific tasks that differ profoundly in various mammalian species (Molnár et al., 2006; Krubitzer, 2007). Thus, fine-tuning neuron numbers in a region- and layer-specific manner is functionally relevant, as also shown by experimental manipulation (Pinto et al., 2009). Our data raise the exciting prospect that long-distance signaling via ChP takes part in such processes during ontogeny and phylogeny by modulating stem cell proliferation at specific times in specific brain regions.

Acknowledgements
We thank Tom Jessell and Kevin Lee for the generous gift of the Gdf7-Cre mice; Andrea Steiner, Angelika Waiser, Detlef Franzen, Julia Niewand and Timucin Öztürk for technical support; and the animal caretakers of the Helmholtz Center Munich for their assistance.

Funding
This work was supported by the Humboldt Foundation Research Fellowship (P.A.J. is a Fellow); the German Research Foundation (DFG); the FP6 Project for the European Transcriptome, Regulome and Cellular Commitment Consortium (EuTRACC) Integrated Project [LSHG-CT-2007-037445] and the Italian Association for Cancer Research (AIRC) [IG 5499]; and in part by the Helmholtz Alliance CoReNe to J.B. and M.G.

Competing interests statement
The authors declare no competing financial interests.

Supplementary material
Supplementary material available online at
http://dev.biologists.org/lookup/suppl/doi:10.1242/dev.090860/-/DC1

References

Acampora, D., Mazan, S., Lallemand, Y., Avantaggiato, V., Maury, M., Simeone, A. and Brûlet, P. (1995). Forebrain and midbrain regions are deleted in Otx2-/- mutants due to a defective anterior neuroectoderm specification during gastrulation. *Development* **121**, 3279-3290.
Acampora, D., Avantaggiato, V., Tuorto, F. and Simeone, A. (1997). Genetic control of brain morphogenesis through Otx gene dosage requirement. *Development* **124**, 3639-3650.
Beazley, K. E., Deasey, S., Lima, F. and Nurminskaya, M. V. (2012). Transglutaminase 2-mediated activation of β-catenin signaling has a critical role in warfarin-induced vascular calcification. *Arterioscler. Thromb. Vasc. Biol.* **32**, 123-130.
Béby, F., Housset, M., Fossat, N., Le Greneur, C., Flamant, F., Godement, P. and Lamonerie, T. (2010). Otx2 gene deletion in adult mouse retina induces rapid RPE dystrophy and slow photoreceptor degeneration. *PLoS ONE* **5**, e11673.
Chenn, A. (2008). Wnt/beta-catenin signaling in cerebral cortical development. *Organogenesis* **4**, 76-80.
Ciaroni, S., Cecchini, T., Ambrogini, P., Buffi, O. and Del Grande, P. (1995). Cell death and cell number in the developing cerebral cortex of MAM treated mice. *J. Hirnforsch.* **36**, 161-170.
Costa, M. R., Wen, G., Lepier, A., Schroeder, T. and Götz, M. (2008). Par-complex proteins promote proliferative progenitor divisions in the developing mouse cerebral cortex. *Development* **135**, 11-22.
Currle, D. S., Cheng, X., Hsu, C. M. and Monuki, E. S. (2005). Direct and indirect roles of CNS dorsal midline cells in choroid plexus epithelia formation. *Development* **132**, 3549-3559.
DasGupta, R. and Fuchs, E. (1999). Multiple roles for activated LEF/TCF transcription complexes during hair follicle development and differentiation. *Development* **126**, 4557-4568.
Diaczok, D., DiVall, S., Matsuo, I., Wondisford, F. E., Wolfe, A. M. and Radovick, S. (2011). Deletion of Otx2 in GnRH neurons results in a mouse model of hypogonadotropic hypogonadism. *Mol. Endocrinol.* **25**, 833-846.
Dziegielewska, K. M., Ek, J., Habgood, M. D. and Saunders, N. R. (2001). Development of the choroid plexus. *Microsc. Res. Tech.* **52**, 5-20.
Ek, C. J., Habgood, M. D., Dziegielewska, K. M. and Saunders, N. R. (2003). Structural characteristics and barrier properties of the choroid plexuses in developing brain of the opossum (Monodelphis Domestica). *J. Comp. Neurol.* **460**, 451-464.
Ek, C. J., Wong, A., Liddelow, S. A., Johansson, P. A., Dziegielewska, K. M. and Saunders, N. R. (2010). Efflux mechanisms at the developing brain barriers: ABC-transporters in the fetal and postnatal rat. *Toxicol. Lett.* **197**, 51-59.
Feil, R., Wagner, J., Metzger, D. and Chambon, P. (1997). Regulation of Cre recombinase activity by mutated estrogen receptor ligand-binding domains. *Biochem. Biophys. Res. Commun.* **237**, 752-757.
Fuchs, J., Stettler, O., Alvarez-Fischer, D., Prochiantz, A., Moya, K. L. and Joshi, R. L. (2012). Engrailed signaling in axon guidance and neuron survival. *Eur. J. Neurosci.* **35**, 1837-1845.
Gato, A. and Desmond, M. E. (2009). Why the embryo still matters: CSF and the neuroepithelium as interdependent regulators of embryonic brain growth, morphogenesis and histiogenesis. *Dev. Biol.* **327**, 263-272.
Götz, M. and Huttner, W. B. (2005). The cell biology of neurogenesis. *Nat. Rev. Mol. Cell Biol.* **6**, 777-788.
Hébert, J. M., Mishina, Y. and McConnell, S. K. (2002). BMP signaling is required locally to pattern the dorsal telencephalic midline. *Neuron* **35**, 1029-1041.
Huang, X., Liu, J., Ketova, T., Fleming, J. T., Grover, V. K., Cooper, M. K., Litingtung, Y. and Chiang, C. (2010). Transventricular delivery of sonic hedgehog is essential to cerebellar ventricular zone development. *Proc. Natl. Acad. Sci. USA* **107**, 8422-8427.
Hunter, N. L. and Dymecki, S. M. (2007). Molecularly and temporally separable lineages form the hindbrain roof plate and contribute differentially to the choroid plexus. *Development* **134**, 3449-3460.
Imayoshi, I., Shimogori, T., Ohtsuka, T. and Kageyama, R. (2008). Hes genes and neurogenin regulate non-neural versus neural fate specification in the dorsal telencephalic midline. *Development* **135**, 2531-2541.
Johansson, P. A., Dziegielewska, K. M., Ek, C. J., Habgood, M. D., Møllgård, K., Potter, A., Schuliga, M. and Saunders, N. R. (2005). Aquaporin-1 in the choroid plexuses of developing mammalian brain. *Cell Tissue Res.* **322**, 353-364.
Johansson, P. A., Dziegielewska, K. M., Ek, C. J., Habgood, M. D., Liddelow, S. A., Potter, A. M., Stolp, H. B. and Saunders, N. R. (2006). Blood-CSF barrier function in the rat embryo. *Eur. J. Neurosci.* **24**, 65-76.
Johansson, P. A., Cappello, S. and Götz, M. (2010). Stem cells niches during development – lessons from the cerebral cortex. *Curr. Opin. Neurobiol.* **20**, 400-407.
Krubitzer, L. (2007). The magnificent compromise: cortical field evolution in mammals. *Neuron* **56**, 201-208.
Landsberg, R. L., Awatramani, R. B., Hunter, N. L., Farago, A. F., DiPietrantonio, H. J., Rodriguez, C. I. and Dymecki, S. M. (2005). Hindbrain rhombic lip is comprised of discrete progenitor cell populations allocated by Pax6. *Neuron* **48**, 933-947.
Lee, K. J., Dietrich, P. and Jessell, T. M. (2000). Genetic ablation reveals that the roof plate is essential for dorsal interneuron specification. *Nature* **403**, 734-740.
Lehtinen, M. K., Zappaterra, M. W., Chen, X., Yang, Y. J., Hill, A. D., Lun, M., Maynard, T., Gonzalez, D., Kim, S., Ye, P. et al. (2011). The cerebrospinal fluid provides a proliferative niche for neural progenitor cells. *Neuron* **69**, 893-905.
Liddelow, S. A., Dziegielewska, K. M., Ek, C. J., Johansson, P. A., Potter, A. M. and Saunders, N. R. (2009). Cellular transfer of macromolecules across the developing choroid plexus of Monodelphis domestica. *Eur. J. Neurosci.* **29**, 253-266.
Marques, F., Sousa, J. C., Coppola, G., Gao, F., Puga, R., Brentani, H., Geschwind, D. H., Sousa, N., Correia-Neves, M. and Palha, J. A. (2011). Transcriptome signature of the adult mouse choroid plexus. *Fluids Barriers CNS* **8**, 10.
Møllgård, K., Milinowska, D. H. and Saunders, N. R. (1976). Lack of correlation between tight junction morphology and permeability properties in developing choroid plexus. *Nature* **264**, 293-294.
Molnár, Z., Métin, C., Stoykova, A., Tarabykin, V., Price, D. J., Francis, F., Meyer, G., Dehay, C. and Kennedy, H. (2006). Comparative aspects of cerebral cortical development. *Eur. J. Neurosci.* **23**, 921-934.
Moon, S. M., Kim, S. A., Yoon, J. H. and Ahn, S. G. (2012). HOXC6 is deregulated in human head and neck squamous cell carcinoma and modulates Bcl-2 expression. *J. Biol. Chem.* **287**, 35678-35688.
Nakamura, T., Colbert, M. C. and Robbins, J. (2006). Neural crest cells retain multipotential characteristics in the developing valves and label the cardiac conduction system. *Circ. Res.* **98**, 1547-1554.
Nielsen, C. M. and Dymecki, S. M. (2010). Sonic hedgehog is required for vascular outgrowth in the hindbrain choroid plexus. *Dev. Biol.* **340**, 430-437.
Ninkovic, J., Pinto, L., Petricca, S., Lepier, A., Sun, J., Rieger, M. A., Schroeder, T., Cvekl, A., Favor, J. and Götz, M. (2010). The transcription factor Pax6 regulates survival of dopaminergic olfactory bulb neurons via crystallin αA. *Neuron* **68**, 682-694.
Omodei, D., Acampora, D., Mancuso, P., Prakash, N., Di Giovannantonio, L. G., Wurst, W. and Simeone, A. (2008). Anterior-posterior graded response to Otx2 controls proliferation and differentiation of dopaminergic progenitors in the ventral mesencephalon. *Development* **135**, 3459-3470.
Parada, C., Escolà-Gil, J. C. and Bueno, D. (2008). Low-density lipoproteins from embryonic cerebrospinal fluid are required for neural differentiation. *J. Neurosci. Res.* **86**, 2674-2684.
Perea-Gomez, A., Rhinn, M. and Ang, S. L. (2001). Role of the anterior visceral endoderm in restricting posterior signals in the mouse embryo. *Int. J. Dev. Biol.* **45**, 311-320.
Pinto, L., Drechsel, D., Schmid, M. T., Ninkovic, J., Irmler, M., Brill, M. S., Restani, L., Gianfranceschi, L., Cerri, C., Weber, S. N. et al. (2009). AP2gamma regulates basal progenitor fate in a region- and layer-specific manner in the developing cortex. *Nat. Neurosci.* **12**, 1229-1237.
Pöschl, J., Grammel, D., Dorostkar, M. M., Kretzschmar, H. A. and Schüller, U. (2012). Constitutive activation of β-Catenin in neural progenitors results in disrupted proliferation and migration of neurons within the central nervous system. *Dev. Biol.* (in press).
Prakash, N., Brodski, C., Naserke, T., Puelles, E., Gogoi, R., Hall, A., Panhuysen, M., Echevarria, D., Sussel, L., Weisenhorn, D. M. et al. (2006). A Wnt1-regulated genetic network controls the identity and fate of midbrain-dopaminergic progenitors in vivo. *Development* **133**, 89-98.

Puelles, E., Acampora, D., Lacroix, E., Signore, M., Annino, A., Tuorto, F., Filosa, S., Corte, G., Wurst, W., Ang, S. L. et al. (2003). Otx dose-dependent integrated control of antero-posterior and dorso-ventral patterning of midbrain. *Nat. Neurosci.* **6**, 453-460.

Puelles, E., Annino, A., Tuorto, F., Usiello, A., Acampora, D., Czerny, T., Brodski, C., Ang, S. L., Wurst, W. and Simeone, A. (2004). Otx2 regulates the extent, identity and fate of neuronal progenitor domains in the ventral midbrain. *Development* **131**, 2037-2048.

Rainer, J., Sanchez-Cabo, F., Stocker, G., Sturn, A. and Trajanoski, Z. (2006). CARMAweb: comprehensive R- and bioconductor-based web service for microarray data analysis. *Nucleic Acids Res.* **34**, W498-W503.

Sugiyama, S., Di Nardo, A. A., Aizawa, S., Matsuo, I., Volovitch, M., Prochiantz, A. and Hensch, T. K. (2008). Experience-dependent transfer of Otx2 homeoprotein into the visual cortex activates postnatal plasticity. *Cell* **134**, 508-520.

R Development Core Team (2005). *R: A Language and Environment for Statistical Computing*. Vienna: R Foundation for Statistical Computing.

von Frowein, J., Wizenmann, A. and Götz, M. (2006). The transcription factors Emx1 and Emx2 suppress choroid plexus development and promote neuroepithelial cell fate. *Dev. Biol.* **296**, 239-252.

Wilting, J. and Christ, B. (1989). An experimental and ultrastructural study on the development of the avian choroid plexus. *Cell Tissue Res.* **255**, 487-494.